

Comparative analysis of whole-body center-of-mass estimation methods in dynamic and static activities using marker-based systems

Jingshu Peng^{a,1}, Mohsen Alizadeh Noghani^{b,1,*}, Edgar Bolívar-Nieto^b

^aXingjian College, Tsinghua University, Beijing, 100084, China

^bAerospace and Mechanical Engineering Department, University of Notre Dame, Notre Dame, 46556, IN, U.S.

Abstract

Accurate estimation of the whole-body center of mass (CoM) is essential for assessing human stability and postural control. However, selecting the most accurate estimation method is challenging due to the complexity of human movement, diverse nature of activities, and varying availability of equipment, such as marker-based systems and ground reaction force (GRF) sensors. This study compares three CoM estimation methods – “Pelvis Markerset”, “Whole-Body Markerset”, and “Whole-Body Markerset & GRFs” – across static activities, such as standing with eyes closed, and dynamic activities, such as picking up an object from the ground. Using the root mean square (RMS) of “external force residual” (the difference between measured ground reaction forces and estimated CoM accelerations multiplied by total body mass) as a performance metric, we found that while all methods performed similarly under static conditions, the “Pelvis Markerset” method showed 96% to 104% higher RMS external force residual values during dynamic activities compared to the two whole-body methods ($p < 0.001$, Cohen’s $d: 2.90-3.04$). The accuracy of “Whole-Body Markerset & GRFs” (i.e., Kalman filter) was similar to “Whole-Body Markerset”, suggesting that incorporating the GRFs through the presented Kalman filter does not improve the estimates from whole-body kinematics. Based on these findings, we recommend the “Whole-Body Markerset” as it performs well and does not require information from GRFs. The “Pelvis Markerset” method can be used in static activities or when markersets around the pelvis reflect whole-body kinematics. This method is not recommended for CoM state estimation in highly dynamic scenarios and when whole-body markersets are available.

1. Introduction

The whole-body center of mass (CoM) is a crucial parameter in the human postural control system and plays a significant role in assessing the stability of human motion (Hof et al., 2005; Corriveau et al., 2001; Schepers et al., 2009). Stability in static conditions is maintained when the vertical projection of the CoM remains within the base of support (BoS) (Winter, 1995). In dynamic conditions (e.g., walking), stability depends not only on the whole-body CoM position

*Corresponding author. Email: malizade@nd.edu.

¹These authors contributed equally to this work and share first authorship.

but also on its velocity (Pai and Patton, 1997). The “extrapolated center of mass” (XCoM) integrates both, predicting the CoM’s future position. Stability is maintained if the XCoM stays within the BoS, providing a margin of stability that helps prevent falls (Hof et al., 2005; Hof, 2008). These principles also apply to legged robots (Kwon and Oh, 2007), where precise CoM control is crucial for maintaining balance. As a result, whole-body CoM estimation is widely used in robotics and human movement research (Cotton et al., 2009; Catena et al., 2018; Burke et al., 2023), particularly in wearable robotics, where it supports balance control strategies (Rajasekaran et al., 2015) and motion planning (Kagawa et al., 2015).

There are two main approaches for estimating whole-body CoM motion, each with its own underlying assumptions. One approach, based on *double integration* of ground reaction forces (GRFs), calculates the CoM position given external forces measured by force plates or sensors (Donelan et al., 2002; Schepers et al., 2009). The second method, referred to as *segment kinematics*, models the body as a chain of rigid segments and estimates the overall CoM by calculating the kinematics of the CoM for one or multiple segments. (Hasan et al., 1996; Pavol et al., 2002; Schepers et al., 2009). Within *segment kinematics*, three main techniques are employed to estimate the CoM position: (1) using the position of one or more markers on the pelvis (Saini et al., 1998), (2) employing a whole-body marker set with anthropomorphic tables to estimate the segment CoM and mass, which can be used to calculate the whole-body CoM (Delp et al., 2007; Dumas et al., 2007; Winter, 2009), and (3) combining the whole-body marker set technique with GRF measurements (Xinjilefu et al., 2015). Due to their popularity and high accessibility of sensor data in contemporary research, we will focus on these three methods, hereon referred to as “Pelvis Markerset”, “Whole-Body Markerset”, and “Whole-Body Markerset & GRFs”.

The primary goal of this study is to compare the effectiveness of the three methods in estimating whole-body CoM position and velocity during 14 distinct activities, including static activities (e.g., standing with eyes closed) and dynamic activities (e.g., picking up an object from the ground). Section 2 outlines the three CoM estimation methods and introduces the “external force residual” as the key performance metric. The root mean square (RMS) of this residual is used to quantify the differences in accuracy across methods. This comprehensive analysis of various activities provides valuable insight into the most suitable estimation method, considering movement complexity and available instrumentation. Section 3 presents the results of CoM position and velocity estimations, while Section 4 offers comparisons and recommendations based on these results. Finally, Section 5 summarizes the key findings.

2. Methods

2.1. Experimental procedure and data collection

We used an existing data set (Alizadeh Noghani and Bolívar-Nieto, 2024) of ten healthy subjects (mean \pm SD, age: 22.9 ± 3.5 years, height: 1.73 ± 0.083 m, mass: 63.66 ± 9.79 kg, 5 males) who provided written informed consent to participate in the study approved by the University of Notre Dame Institutional Review Board (Protocol ID: 24-01-8277).

The subjects were fitted with fifty-seven reflective markers following a whole-body marker set (OptiTrack, 2022) (Fig. 1). Then, they performed a series of 14 activities, each repeated three times, based on the Berg Balance Scale test (Berg et al., 1992) over a walkway instrumented with force plates (Table 1). Based on the magnitude of displacement of body segments, the activities were qualitatively classified as Static or Dynamic.

During experiments, the force plates (Kistler Instrumente AG, Winterthur, Switzerland) recorded 3D GRFs at 1000 Hz, while a twelve-camera motion capture system (PrimeX22, NaturalPoint

Table 1: The list of activities performed by participants and the provided instructions. The activities marked with † are in the Static group, while others are considered Dynamic. Shaded activities are similar to those in the Berg Balance Scale test. This table has been reproduced from our previous work (Alizadeh Noghani and Bolívar-Nieto, 2024).

Activity	Description
(1) Sit to Stand	Stand up from the chair without using your hands for support.
(2) Stand to Sit	Sit down on the chair without using your hands for support.
(3) Foot on Chair	Place your right foot on the upper surface of the chair in front of it. The left foot replicates this motion but is not placed on the chair. Repeat for four cycles.
(4) Stride	Take a stride forward, then stop.
(5) Look Behind†	Turn to look directly behind, first over your left shoulder, and then your right shoulder.
(6) Feet Together†	Stand with your feet placed as close together as possible.
(7) Eyes Closed†	Stand still with your eyes closed.
(8) Turn	Turn 180°, pause, then turn back to your original direction.
(9) Tandem Feet†	Stand with one foot directly in front of the other, with your feet as close together as possible.
(10) One Leg	Stand on one leg, then return to neutral pose.
(11) Squat	Perform a squat, then return to neutral pose.
(12) Reach Forward	Reach forward as much as possible while keeping your arms parallel, then return to neutral pose.
(13) Object Pickup	Pick up an object placed in front of your right foot.
(14) Shoe Lace	Step down to emulate tying your right shoe laces, then return to neutral pose.

Inc., OR, USA) simultaneously captured the marker positions at 200 Hz. The marker data was processed using Motive 3.0 (NaturalPoint Inc., OR, USA) and lowpass-filtered at 6 Hz. Force-plate data was lowpass-filtered using a 5th order Butterworth filter (cutoff frequency of 20 Hz) and then downsampled to 200 Hz. Subsequent analysis was performed in MATLAB (MathWorks Inc., MA, USA) and OpenSim (Delp et al., 2007). The One Leg, Squat, and Shoe Lace trials were split into two parts, capturing the movements at the start and return phases of the movement.

2.2. CoM state estimation

We employed three methods to estimate the CoM position and velocity. For the Pelvis Markerset (*PM*) method, the CoM position was calculated by averaging the positions of four pelvic markers: RIAS, LIAS, LIPS, and RIPS (Fig. 1a) (Saini et al., 1998). The CoM velocity was obtained by applying central finite differences to the CoM position.

For the Whole-Body Markerset (*WM*) method, we modified a full-body OpenSim model (Rajagopal et al., 2016) by adding a separate head-and-neck segment connected to the torso with three rotation degrees of freedom. The segment’s mass and CoM position were derived from the anthropometric tables (Dumas et al., 2007). After performing inverse kinematics, the whole-body CoM position and velocity were obtained using OpenSim’s BodyKinematics analysis tool (Seth et al., 2011; Sherman et al., 2011).

Lastly, the Whole-Body Markerset & GRFs (*WMG*) method fused the *WM* estimates with GRFs to compute the CoM position and velocity (Xinjilefu et al., 2015). The dynamics of the

CoM were modeled as follows,

$$x[k] = Ax[k-1] + Bu[k-1] + w[k], \quad (1)$$

$$y[k] = Cx[k] + v[k], \quad (2)$$

$$A = \begin{bmatrix} 1 & \Delta T & 0 & 0 & 0 & 0 \\ 0 & 1 & 0 & 0 & 0 & 0 \\ 0 & 0 & 1 & \Delta T & 0 & 0 \\ 0 & 0 & 0 & 1 & 0 & 0 \\ 0 & 0 & 0 & 0 & 1 & \Delta T \\ 0 & 0 & 0 & 0 & 0 & 1 \end{bmatrix}, B = \begin{bmatrix} \frac{\Delta T^2}{2} & 0 & 0 \\ \Delta T & 0 & 0 \\ 0 & \frac{\Delta T^2}{2} & 0 \\ 0 & \Delta T & 0 \\ 0 & 0 & \frac{\Delta T^2}{2} \\ 0 & 0 & \Delta T \end{bmatrix}, C = \begin{bmatrix} 1 & 0 & 0 & 0 & 0 & 0 \\ 0 & 0 & 1 & 0 & 0 & 0 \\ 0 & 0 & 0 & 0 & 1 & 0 \end{bmatrix}, \quad (3)$$

where $x \in \mathbf{R}^6$ represents the 3D components of the CoM position (i.e., x_1, x_3 , and x_5) and velocity (i.e., x_2, x_4 , and x_6), which are to be estimated; $u \in \mathbf{R}^3$ is the acceleration of the CoM computed from GRFs measured by the force plates; and $y \in \mathbf{R}^3$ is the nonsmoothed CoM position given by *WM*. A is the state transition dynamics, B is the influence of control inputs on the state, C is the mapping from the states to observed outputs (i.e., CoM position), and $\Delta T = 5 \text{ ms}$ is the sample time. We assumed that the process and measurement noise ($w[k] \sim \mathcal{N}(0, V_w)$ and $v[k] \sim \mathcal{N}(0, V_v)$) follow a normal distribution with zero mean and process and measurement covariance matrices V_w and V_v . We applied a Kalman filter to estimate $x[k]$. A genetic algorithm that minimized the difference between the *WMG* and low-pass-filtered *WM* estimates (with a cutoff frequency of 6 Hz) specified the process and measurement covariance matrices, V_w and V_v .

The accuracy of these methods in estimating CoM position and velocity was quantitatively evaluated using the ‘‘external force residual’’, $r(t) \in \mathbf{R}^3$, defined as

$$r(t) = F_{ext}(t) - ma_{est}(t), \quad (4)$$

where $F_{ext}(t)$ represents the net external force at time t , m is the participant’s mass, and a_{est} is the estimated acceleration. This residual measures the discrepancy between the net external force, computed by subtracting gravitational force from the force plate measurements, and the estimated net external force based on the acceleration given by the three estimation methods, providing a metric for assessing their accuracy. We used the ‘‘external force residual’’ because the experimental GRFs divided by total mass were the closest available measurement to a ‘‘ground truth’’ for CoM kinematics.

To minimize the noise that was introduced during the estimation process, a smoothing technique minimized both the norm of the signal fit error and the third derivative of the signal (Yazdani et al., 2012), as formulated by the following optimization problem,

$$\min_{\hat{x}} \|x - \hat{x}\|_2^2 + \alpha \|D_3 \hat{x}\|_2^2, \quad (5)$$

where x is the original signal, \hat{x} is the filtered signal, $\|\cdot\|_2^2$ is the L^2 -norm, and D_3 denotes the third derivative; therefore, $\|D_3 \hat{x}\|_2^2$ penalizes the CoM jerk when applied to the position signal, and CoM snap when applied to the velocity signal, with the tunable parameter α controlling the trade-off between signal fit and jerk or snap minimization (Boyd and Vandenberghe, 2004). Through experimentation, a value of 300 for α was found to balance smoothing the signal while preserving local features. For all three methods, following the smoothing process, a_{est} was obtained by applying central finite differences for numerical differentiation.

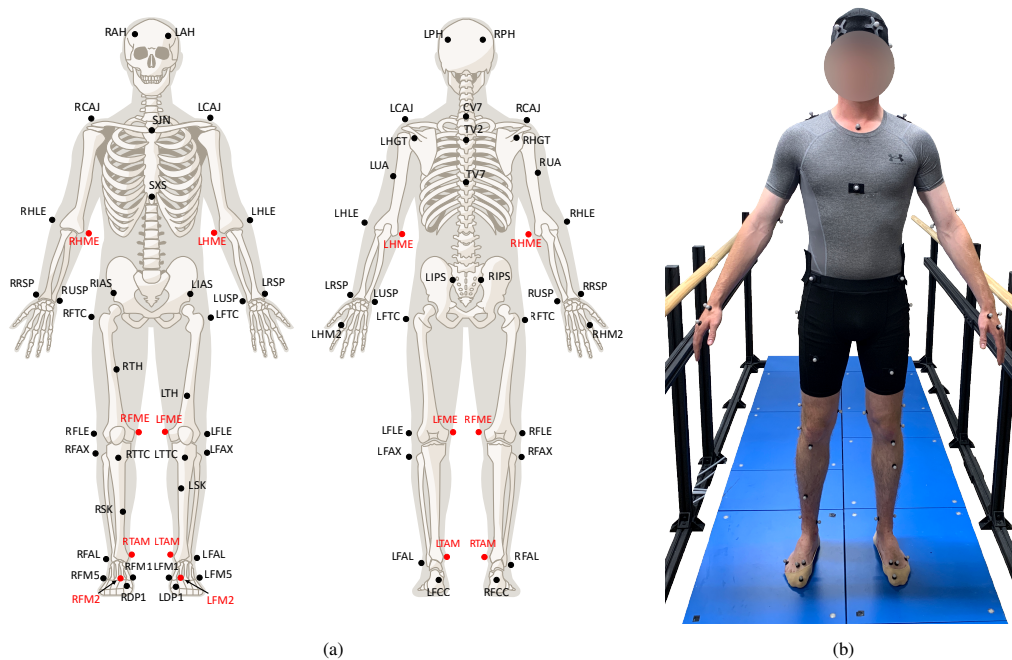


Fig. 1: (a) The anterior and posterior views of the Biomech (57) marker set. The calibration markers are highlighted in red. (b) A participant fitted with the marker set, standing in an A-pose on the instrumented walkway.

After computing the residual $r(t)$, we compared the performance of the methods by averaging the RMS of $r(t)$ along the three dimensions and subsequently the three repeats of each activity. The normality of the data was verified using Q-Q plots. One-way analysis of variance (ANOVA) was used to identify if the estimation method was a main effect and post-hoc t-tests with Bonferroni correction were performed to detect pairwise differences. Significance level (α) was set to 0.05 and eta-squared (η^2) and point estimate of Cohen's d , along with its 95% confidence interval (95% CI) quantified effect sizes; magnitudes d of 0.2, 0.5, and 0.8 were considered as thresholds for small, medium, and large effects, respectively (Cohen, 1988).

3. Results

ANOVA did not identify a significant difference among the three methods when estimating position in the Static activities ($p = 0.730$) (Fig. 2a and 2b). However, there was a main effect of estimation method in the Dynamic activities ($p < 0.001$, $\eta^2 = 0.74$). Post-hoc tests identified significant differences between all three pairs of $WMG - WM$ ($p < 0.001$, $d = 0.01$, 95% CI = $(-0.82, 0.85)$), $WMG - PM$ ($p < 0.001$, $d = -2.90$, 95% CI = $(-4.15, -1.63)$), and $WM - PM$ ($p < 0.001$, $d = -2.91$, 95% CI = $(-4.16, -1.63)$).

For CoM velocity, while there was no main effect of the estimation method in the Static group ($p = 0.791$), the difference in the Dynamic activities was significant ($p < 0.001$, $\eta^2 = 0.76$) (Fig. 2c and 2d). Subsequent t-tests revealed differences between $WMG - PM$ ($p < 0.001$, $d = 3.04$, 95% CI = $(-4.32, -1.73)$) and $WM - PM$ ($p < 0.001$, $d = 2.99$, 95% CI = $(-4.33, -1.69)$) pairs, but not between $WMG - WM$ ($p = 0.066$).

4. Discussion

4.1. Comparison of the CoM estimation methods

When estimating position in Static activities, there is no method among the three that outperforms the others. This was expected because in the four activities in the Static group (Look Behind, Feet Together, Eyes Closed, and Tandem Feet), the participants remained upright and the body segments did not move significantly. As a result, the CoM remained close to the center of pelvis, and the PM method captured the CoM kinematics with similar accuracy to the other two methods. In contrast, in the Dynamic activities, PM performed worse than the other two methods, with the average RMS residual being 96% higher than WM (Fig. 2a). This trend was consistent across all the dynamic activities (Fig. 2b); the PM method does not include information about the movement of the upper or lower body, which experienced large displacements in the Dynamic activities such as Shoe Lace, resulting in the large RMS values. Interestingly, the RMS of residual of WMG was consistently and slightly worse than WM across all activities, with a 0.28% higher average. However, the effect size was negligible ($d = 0.01$) and its 95% CI covered zero, suggesting that this may not translate to a difference in the performance of the estimators.

The results for velocity estimations were similar to position, albeit with no difference between the two whole-body methods in the Dynamic activities (Fig. 2c). We note that the WMG had a larger RMS than the pelvis-based method in Eyes Closed and Feet Together activities (Fig. 2d). This may be due to the Kalman filter estimate converging to a velocity estimate with a small offset from 0 in these Static trials, resulting in increased RMS residual force in the process.

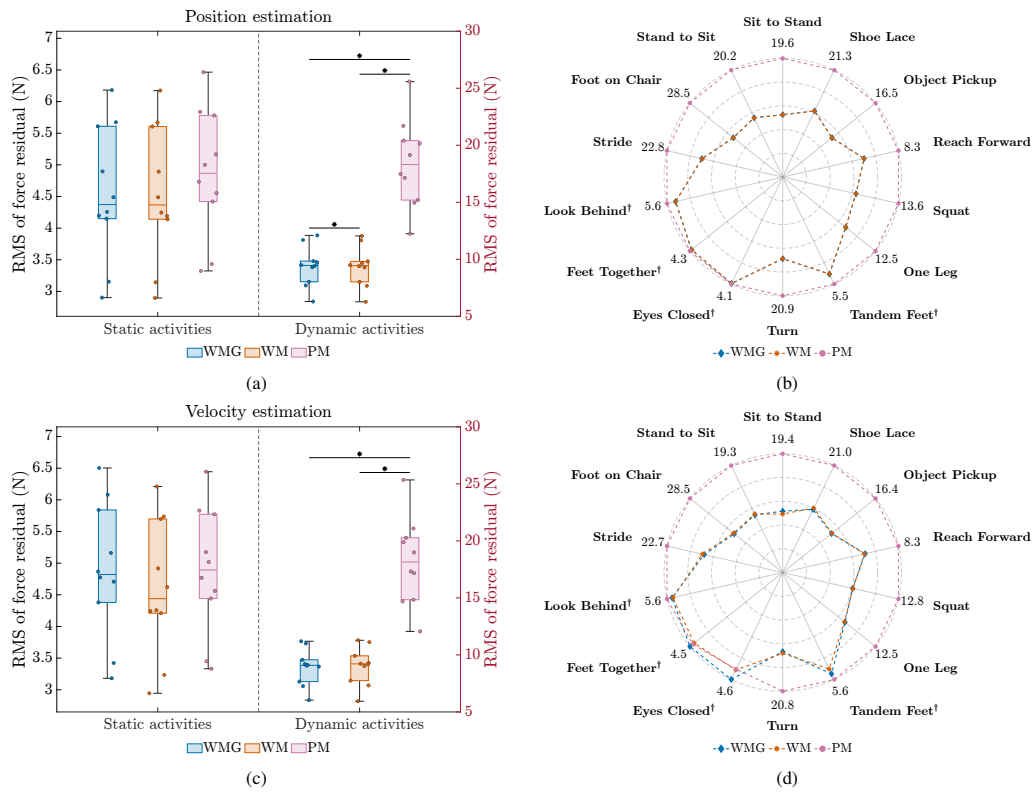


Fig. 2: (a,c) RMS of force residual for Static and Dynamic activities, when estimating position and velocity. The * symbols denote statistical significance in the post-hoc tests. (b,d) The average RMS of force residual for the 14 activities; the four activities in the Static group are denoted by †. The axis limits represent the maximum RMS residual among the methods in each activity.

4.2. Recommendations for the CoM estimation methods

The results suggest that incorporating GRFs through the presented Kalman filtering framework does not produce a more accurate estimate over the *WM* method. Therefore, to estimate the CoM position and velocity, the *WM* method is recommended for its consistent accuracy across all activities. In resource-limited situations, the *PM* can be a feasible option for static activities. However, its performance gap with the whole-body kinematics methods became more pronounced with increased CoM movement. In particular, when substantial CoM displacement was involved, this disparity was large (Fig. 2b and 2d). Therefore, caution is required when interpreting the CoM state estimation results in dynamic activities using the *PM* method.

5. Conclusion

Our study compared three CoM position and velocity estimation methods across 14 distinct activities in 3D by assessing their accuracy through the RMS of “external force residual”. The results show the whole-body marker set delivers accurate estimates across all the activities, while those based on the pelvis marker set are mainly effective in static activities. Further, fusing the estimates from the whole-body marker set with the GRFs by using a Kalman filter did not improve the estimation. These findings across a diverse array of movements provide practical recommendations for selecting a CoM estimation method tailored to the dynamics of the movement.

References

- Alizadeh Noghani, M., Bolívar-Nieto, E., 2024. Predicting center of mass position in non-cyclic activities: The influence of acceleration, prediction horizon, and ground reaction forces. doi:10.48550/ARXIV.2411.16891.
- Berg, K.O., Wood-Dauphinee, S.L., Williams, J.I., Maki, B., 1992. Measuring balance in the elderly: Validation of an instrument. *Canadian Journal of Public Health = Revue Canadienne De Sante Publique* 83 Suppl 2, S7–11.
- Boyd, S., Vandenberghe, L., 2004. *Convex Optimization (Chapter 6.3)*. Cambridge University Press.
- Buurke, T.J., Van De Venis, L., Den Otter, R., Nonnekens, J., Keijsers, N., 2023. Comparison of ground reaction force and marker-based methods to estimate mediolateral center of mass displacement and margins of stability during walking. *Journal of Biomechanics* 146, 111415. doi:10.1016/j.jbiomech.2022.111415.
- Catena, R.D., Connolly, C.P., McGeorge, K.M., Campbell, N., 2018. A comparison of methods to determine center of mass during pregnancy. *Journal of Biomechanics* 71, 217–224. doi:10.1016/j.jbiomech.2018.02.004.
- Cohen, J., 1988. *Statistical Power Analysis for the Behavioral Sciences*. 2 ed., Routledge. doi:10.4324/9780203771587.
- Corriveau, H., Hébert, R., Prince, F., Raïche, M., 2001. Postural control in the elderly: An analysis of test-retest and interrater reliability of the COP-COM variable. *Archives of Physical Medicine and Rehabilitation* 82, 80–85. doi:10.1053/apmr.2001.18678.
- Cotton, S., Murray, A., Fraisse, P., 2009. Estimation of the Center of Mass: From Humanoid Robots to Human Beings. *IEEE/ASME Transactions on Mechatronics* 14, 707–712. doi:10.1109/TMECH.2009.2032687.
- Delp, S.L., Anderson, F.C., Arnold, A.S., Loan, P., Habib, A., John, C.T., Guendelman, E., Thelen, D.G., 2007. OpenSim: Open-Source Software to Create and Analyze Dynamic Simulations of Movement. *IEEE Transactions on Biomedical Engineering* 54, 1940–1950. doi:10.1109/TBME.2007.901024.
- Donelan, J., Kram, R., Kuo, A.D., 2002. Simultaneous positive and negative external mechanical work in human walking. *Journal of Biomechanics* 35, 117–124. doi:10.1016/S0021-9290(01)00169-5.
- Dumas, R., Chèze, L., Verriest, J.P., 2007. Adjustments to McConville et al. and Young et al. body segment inertial parameters. *Journal of Biomechanics* 40, 543–553. doi:10.1016/j.jbiomech.2006.02.013.
- Hasan, S.S., Robin, D.W., Szurkus, D.C., Ashmead, D.H., Peterson, S.W., Shiavi, R.G., 1996. Simultaneous measurement of body center of pressure and center of gravity during upright stance. Part I: Methods. *Gait & Posture* 4, 1–10. doi:10.1016/0966-6362(95)01030-0.
- Hof, A., Gazendam, M., Sinke, W., 2005. The condition for dynamic stability. *Journal of Biomechanics* 38, 1–8. doi:10.1016/j.jbiomech.2004.03.025.
- Hof, A.L., 2008. The ‘extrapolated center of mass’ concept suggests a simple control of balance in walking. *Human Movement Science* 27, 112–125. doi:10.1016/j.humov.2007.08.003.

- Kagawa, T., Ishikawa, H., Kato, T., Sung, C., Uno, Y., 2015. Optimization-Based Motion Planning in Joint Space for Walking Assistance With Wearable Robot. *IEEE Transactions on Robotics* 31, 415–424. doi:10.1109/TR0.2015.2409434.
- Kwon, S., Oh, Y., 2007. Estimation of the center of mass of humanoid robot, in: 2007 International Conference on Control, Automation and Systems, IEEE, Seoul, South Korea. pp. 2705–2709. doi:10.1109/ICCAS.2007.4406826.
- OptiTrack, 2022. Biomech 57 markerset - movement sciences documentation. <https://docs.optitrack.com/movement-sciences/movement-sciences-marker-sets/biomech-57>. Accessed: 2024-10-25.
- Pai, Y.C., Patton, J., 1997. Center of mass velocity-position predictions for balance control. *Journal of Biomechanics* 30, 347–354. doi:10.1016/S0021-9290(96)00165-0.
- Pavol, M.J., Owings, T.M., Grabiner, M.D., 2002. Body segment inertial parameter estimation for the general population of older adults. *Journal of Biomechanics* 35, 707–712. doi:10.1016/S0021-9290(01)00250-0.
- Rajagopal, A., Dembia, C.L., DeMers, M.S., Delp, D.D., Hicks, J.L., Delp, S.L., 2016. Full-Body Musculoskeletal Model for Muscle-Driven Simulation of Human Gait. *IEEE Transactions on Biomedical Engineering* 63, 2068–2079. doi:10.1109/TBME.2016.2586891.
- Rajasekaran, V., Aranda, J., Casals, A., Pons, J.L., 2015. An adaptive control strategy for postural stability using a wearable robot. *Robotics and Autonomous Systems* 73, 16–23. doi:10.1016/j.robot.2014.11.014.
- Saini, M., Kerrigan, D.C., Thirunarayan, M.A., Duff-Raffaele, M., 1998. The Vertical Displacement of the Center of Mass During Walking: A Comparison of Four Measurement Methods. *Journal of Biomechanical Engineering* 120, 133–139. doi:10.1115/1.2834293.
- Schepers, H., Van Asseldonk, E., Buurke, J., Veltink, P., 2009. Ambulatory Estimation of Center of Mass Displacement During Walking. *IEEE Transactions on Biomedical Engineering* 56, 1189–1195. doi:10.1109/TBME.2008.2011059.
- Seth, A., Sherman, M., Reinbolt, J.A., Delp, S.L., 2011. OpenSim: A musculoskeletal modeling and simulation framework for in silico investigations and exchange. *Procedia IUTAM* 2, 212–232. doi:10.1016/j.piutam.2011.04.021.
- Sherman, M.A., Seth, A., Delp, S.L., 2011. Simbody: Multibody dynamics for biomedical research. *Procedia IUTAM* 2, 241–261. doi:10.1016/j.piutam.2011.04.023.
- Winter, D., 1995. Human balance and posture control during standing and walking. *Gait & Posture* 3, 193–214. doi:10.1016/0966-6362(96)82849-9.
- Winter, D.A., 2009. *Biomechanics and Motor Control of Human Movement*. 1 ed., Wiley. doi:10.1002/9780470549148.
- Xinjilefu, X., Feng, S., Atkeson, C.G., 2015. Center of mass estimator for humanoids and its application in modelling error compensation, fall detection and prevention, in: 2015 IEEE-RAS 15th International Conference on Humanoid Robots (Humanoids), IEEE, Seoul, South Korea. pp. 67–73. doi:10.1109/HUMANOIDS.2015.7363533.
- Yazdani, M., Gamble, G., Henderson, G., Hecht-Nielsen, R., 2012. A simple control policy for achieving minimum jerk trajectories. *Neural Networks* 27, 74–80. doi:10.1016/j.neunet.2011.11.005.